Austin Journal of Radiology

Open Access

Austin Publishing Group

Research Article

Usefulness and Consideration of Multi-Band EPI using Simultaneous Multi-Slice for Diffusion Kurtosis Imaging at 1.5 Tesla Magnetic Resonance Imaging

Akihiro Kasahara[1,2]*, Yuiti Suzuki[1], Minoru Mitsuda[1], Kohki Yoshikawa[2], Masaaki Hori[3], Katsuya Maruyama[4], Yasushi Watanabe[1], Akira Kunimatsu[1], Keiichi Yano[1] and Osamu Abe[1]

[1]Department of Radiology, University of Tokyo Hospital, Japan

[2]Graduate Division of Health Sciences, Komazawa University, Japan

[3]Department of Radiology, Juntendo University School of Medicine, Japan

[4]SIEMENS Japan K.K, Japan

***Corresponding author:** Akihiro Kasahara, Department of Radiology, University of Tokyo Hospital and Graduate Division of Health Sciences, Komazawa University, Bunkyo-ku, Tokyo, Japan

Received: September 22, 2016; **Accepted:** October 18, 2016; **Published:** October 20, 2016

Abstract

Multiband Echo Planar Imaging (MB-EPI) was developed as a sequence for the Human Connectome Project of a large-scale clinical trial in the US. Recently, the concomitant use of MB-EPI with functional Magnetic Resonance Imaging (MRI) or diffusion MRI was reported; however, the combination of MB-EPI with Diffusional Kurtosis Imaging (DKI) has not been reported. We investigated the characteristics of Mean Kurtosis (MK) when MB-EPI was applied to DKI in a clinical 1.5 Tesla MRI. We obtained two DKIs, one of an MB-short when acquisition time was shortened and one of an MB-Motion Probing Gradient (MPG) with an increased number of directions at acquisition, similar to a conventional DKI by MB-EPI. These were compared to the reference DKI. An MK map or a quantitative value map of DKI and a tractography of a pyramidal tract were prepared. The latter was designated as the volume of interest, and a tract-specific analysis was conducted to detect statistically significant differences in MK values. When MB-EPI was used (MB-short and MB-MPG), the mean MK value of the pyramidal tract decreased compared to the reference DKI, and both were statistically significant from the DKI. Unlike other studies, we used a 12-channel receiver coil in a 1.5 Tesla MRI. Because the properties of the coil and MRI equipment adversely affect image reconstruction accuracy, this might have led to the statistical significance that we found. Equipment specifications in the imaging environment should be considered when carrying out quantitative evaluations.

Keywords: Multi-band EPI; Simultaneous multi-slice; DWI; DKI; Non-Gaussian diffusion

Abbreviations

MRI: Magnetic Resonance Imaging; DKI: Diffusional Kurtosis Imaging; MK: Mean Kurtosis; MPG: Motion Probing Gradient; DWI: Diffusion Weighted Imaging; QSI: Q-Space Imaging; GRAPPA: Generalized Autocalibrating Partially Parallel Acquisition; MB-factor: Multiband factor; FA: Fractal Anisotropy; ROI: Region Of Interest; VOI: Volume Of Interest; TSA: Tract-Specific Analysis; TR: Repetition Time; L-factor: Leakage factor; SNR: Signal-To-Noise Ratio; g-factor: geometry factor

Introduction

Diffusion-Weighted Imaging (DWI) capturing the signal of the water molecule has been widely applied to collect detailed information of the brain such as extraction of nerve fiber [1-3]. Most water molecule diffusion in vivo hits various endothelial cells, making this restricted diffusion [4,5]. Therefore, DWI can express, to some extent, the characteristics of the diffusion phenomenon in vivo. Recent studies have used techniques, such as Q-Space Imaging (QSI) and Diffusional Kurtosis Imaging (DKI), that express restricted diffusion [6,7]. DKI expresses quantitatively how a water molecule deviates from free diffusion and reportedly can evaluate the actual in vivo fine structure more clearly than DWI. Moreover, clinical application of non-Gaussian diffusion MRI [8] is easier compared with QSI, since imaging at several b-values are available. Raab et al. reported that differential grading of glioma was available in DKI [9]. Acquisition time is longer due to an increased Motion Probing Gradient (MPG) and imaging at multiple b-values (Raab's DKI is 11 min 57 sec [9]). As a representative technique to accelerate acquisition time in-plane, parallel imaging [10]. On the contrary, the technique of Multiband Echo Planar Imaging (MB-EPI) [11,12] developed in the Human Connective Project [13] with characteristics to shorten acquisition time along the slice direction is now available in clinical equipment. With this technique, multiple slices are simultaneously excited to obtain overwrapped image data; subsequently, these data are separated in individual slice data, using the differences of many coil sensitivities [11]. The clinical application of MB-EPI has been reported [14,15]. In this study, we aimed to investigate the points we should note and the changes appearing in the images when used in combination with DKI and MB-EPI as use in conventional DKI.

Material and Methods

Subjects

Subjects were 13 healthy male volunteers (mean age 29.0 ± 5.39 years). This study was previously approved by the institutional ethics committees of the University of Tokyo Hospital and Komazawa University, and only subjects who signed the written informed consent alone were included in the study.

Citation: Kasahara A, Suzuki Y, Mitsuda M, Yoshikawa K, Hori M, Maruyama K, et al. Usefulness and Consideration of Multi-Band EPI using Simultaneous Multi-Slice for Diffusion Kurtosis Imaging at 1.5 Tesla Magnetic Resonance Imaging. Austin J Radiol. 2016; 3(4): 1060.

Table 1: Comparison of imaging conditions.

	ref.DKI	MB-short	MB-MPG
TR / TE [ms]	7810/92	4500/87	4500/87
number of MPG directions	30	30	50
multi-band factor	1	2	2
aquitision time [min:sec]	8:20	5:14	8:14

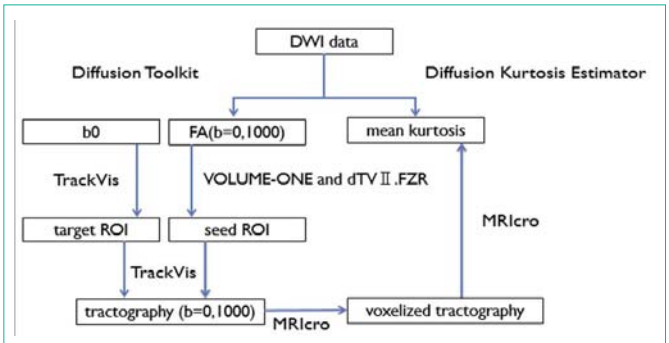

Figure 1: VOI drawing of pyramidal tract to be used in TSA.

Equipment and imaging conditions

All MR imaging were performed on a 1.5 Tesla MR scanner (MAGNETOM Avanto, Siemens, Munich, Bavaria, German). Three imaging methods were compared: the conventional method without MB-EPI, which was used as the reference DKI (ref. DKI); a combined MB-EPI with ref. DKI to shorten the acquisition time (MB-short); and MB-MPG with an increased number of MPG directions (50 directions) to obtain a similar acquisition time as the ref. DKI. The version of the MB-EPI sequence used in this study was Release R012 (https://www.cmrr.umn.edu/multiband/#refs). The common parameters for individual imaging included the following: single-shot SE-EPI, FOV 24.5 × 24.5 cm^2, matrix size 98 × 98, slice thickness 2.5 mm, slice gap 0 mm, slice sections 60, b-values 0, 1000, and 2000 s/mm^2, δ/Δ 32.7/37.4 msec, generalized autocalibrating partially parallel acquisition (GRAPPA) acceleration factor 2, and an average of 1. In comparison, the Multiband factor (MB-factor) in MB-short and MB-MPG was set at 2. The speed-up level along the slice direction in MB-EPI is called a MB-factor. The parameters are shown in Table 1.

Analysis

Figure 1 shows the analysis process. The distortion of all DWI data was corrected using FSL 4.0 (http:// fsl.fmrib.ox.ac.uk/fsl/fsl4.0/feat5/detail.html). Fractal Anisotropy (FA) was estimated using the Diffusion Toolkit (http://www.trackvis.org/dtk/) from the DWI data at b = 0 and 1000 sec/mm^2 obtained from DKI. The seed Region Of Interest (ROI) was set at the cerebral peduncle on the FA map, using TrackVis (http://www.trackvis.org). The target ROI was set at the primary motor cortex at b = 0 in the ref. DKI, using VOLUME-ONE and dTV II.FZR (developed by Masutani et al., Information Science, Hiroshima City University). Tractography of the pyramidal tract was drawn using these ROIs and TrackVis (Figure 2a). The second-order RungeKutta method was used for the tractography algorithm and the initial value settings for the other parameters. The tractography was voxelized, and the Volume Of Interest (VOI) was drawn using MRIcro (http://www.mccauslandcenter.sc.edu/mricro/mricro/mricro. html) (Figure 2b). Based on the DWI data obtained from individual imaging, kurtosis analysis was conducted to draw the Mean Kurtosis (MK) map, using Diffusion Kurtosis Estimator (https://www.nitrc.org/projects/dke). MK, as the quantitative value, expresses

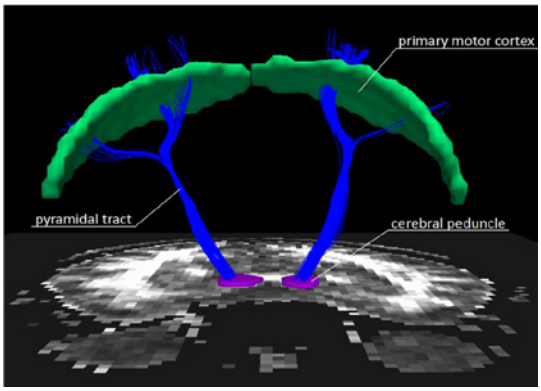

Figure 2a: Tractography of pyramidal tract prepared with TrackVis.
In this Figure, seed ROI was set using TrackVis at the left and right cerebral peduncles, and the pyramidal tract from this point to the primary motor cortex was drawn. This primary motor cortex was drawn using VOLUME-ONE and dTVII.FZR.

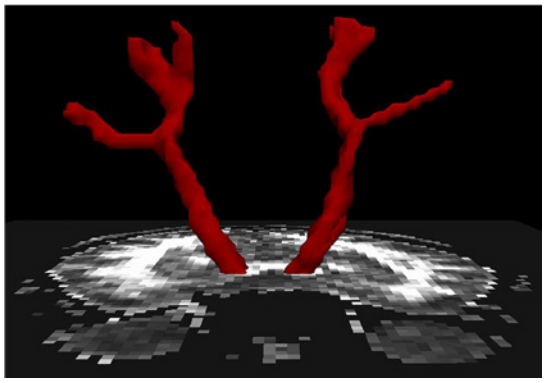

Figure 2b: VOI voxelized the tractography of pyramidal tract.
The tractography of the pyramidal tract obtained in Fig 1a was voxelized and displayed on TrackVis.

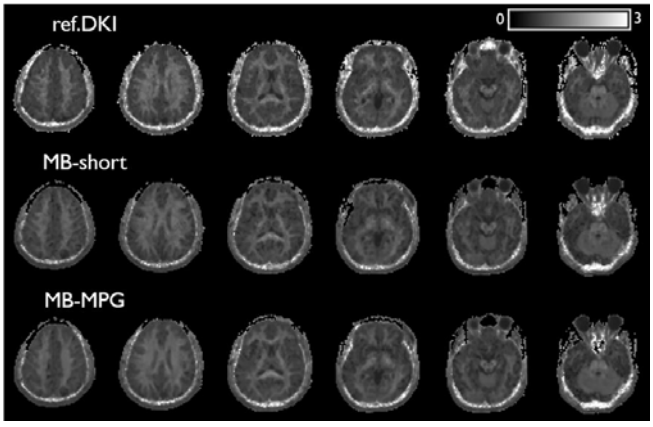

Figure 3: Mean kurtosis (MK) map obtained by each imaging method.
In MK map obtained by imaging method used MB-EPI (MB-short and MB-MPG), apparent artifact and image degradation were not visually observed. Acquisition time was 8 min 20 sec for reference DKI, 5 min 14 sec for MB-short, and 8 min 14 sec for MB-MPG, respectively.

Table 2: Mean values of the mean kurtosis of pyramidal tract in subjects, obtained from individual imaging.

		ref.DKI		MB-short		MB-MPG	
Case	Age	Right	Left	Right	Left	Right	Left
1	28	1.2205	1.2942	1.0757	1.177	1.1034	1.1861
2	26	1.0211	1.1923	1.0042	1.1328	0.9859	1.1402
3	25	1.0548	1.1966	1.0309	1.1557	1.0247	1.1128
4	33	1.1802	1.1619	1.1087	1.0849	1.0941	1.1024
5	32	1.2169	1.2063	1.1383	1.1107	1.0909	1.1024
6	29	1.1905	1.2011	1.1435	1.196	1.1206	1.1103
7	25	1.1445	1.1636	1.2022	1.2807	1.1445	1.1636
8	24	1.1501	1.134	1.1106	1.0634	1.1138	1.0874
9	24	1.214	1.1974	1.1741	1.112	1.1224	1.0568
10	25	1.138	1.219	1.0942	1.1698	1.104	1.192
11	27	1.1083	1.2182	1.0732	1.1534	1.0681	1.1529
12	32	1.1001	1.112	1.0119	1.0251	0.9803	1.0036
13	30	1.1037	1.2393	1.0398	1.1413	1.0632	1.1745

the mean of diffusion kurtosis against each MPG direction. Tract-Specific Analysis (TSA) [16] was conducted using this MK map and the VOI of the pyramidal tract, and statistically significant differences among the imaging conditions were analyzed by Dennett's test.

Results

The MK map obtained from each imaging is shown in Figure 3. The acquisition time in MB-short with MB-EPI was reduced to 37.2% (8 min 20 sec→5 min 14 sec) compared to the ref. DKI. Mean ± standard deviation of the MK obtained by images of 26 patterns of left and right pyramidal tracts in 13 subjects was 1.1684 ± 0.0594 for ref. DKI, 1.1158 ± 0.0646 for MB-short, and 1.1000 ± 0.0555 for MB-MPG (Table 2, Figure 4). Significant differences from the ref. DKI were observed in MB-short (p = 0.0052) and MB-MPG (p=0.0003).

Discussion

Although we used an MB-factor of 2, the minimum Repetition Time (TR) may be much less if a higher MB-factor is used. This would result in a shorter acquisition time. Under this condition, however, excitation will progress next in the state holding insufficient longitudinal relaxation of the water molecule, and the observed signals will be attenuated. For this reason, the best time for sufficient longitudinal relaxation should be selected for the TR. Consequently, the minimum RT reduced by using MB-EPI may not always be feasible, and an appropriate MB-factor should be selected when MB-EPI is used.

In the separation of slices in MB-EPI, the signal attenuates in the inherent slice, and the signals of other slices are combined and become noise [17]. The degree of this incomplete separation of slices is presented as a Leakage factor (L-factor) that increases with an increasing MB-factor [18]. We found that MB-EPI decreased the mean signal value of the pyramidal tract. This may have been due to an incomplete separation of slices, but our results showed the same tendency as those reported by Kamil et al. [17].

Parallel imaging was used for the imaging condition in this

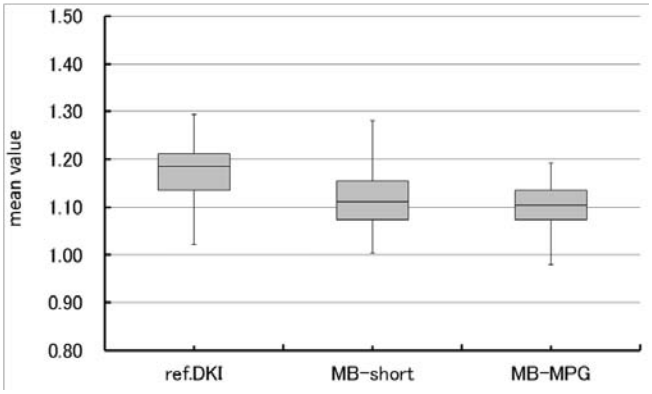

Figure 4: Mean values of the mean kurtosis of pyramidal tract obtained from individual imaging.

study. With this method, a decreased Signal-To-Noise Ratio (SNR) or increased geometry factor (g-factor) is observed with an increased reduction factor, indicating the degree of in-plane acceleration. The g-factor indicates image deterioration when image data are developed.

The GRAPPA method is used in parallel imaging [12]. Xu et al. applied GRAPPA to the separation of slices in MB-EPI [19]. Consequently, the g-factor will be more elevated by this concomitant use. Our results showed a similar tendency to the results reported by Xu et al. since we also used the GRAPPA method for parallel imaging in combination with MB-EPI. Another method shifts the overwrapped slices to the direction of the phase in MB-EPI to decrease the L-factor [18]; however, the shifted overwrapped slices turn down in the plane due to the phase-encode decrease by parallel imaging, and aliasing is generated [20] so that the effect to shift the image to the direction of the phase is attenuated. Therefore, balancing the individual factors of MB-EPI and parallel imaging is essential.

Wiggins et al. [21] suggested that imaging is accelerated if there are more elements in a receiver coil. They are similarly observed at the direction of the slice [19]. Wiggins et al. compared g-factors using receiver coils having 96, 32, and 12 channels in a 3 Tesla MRI [21]. When there are fewer elements, the g-factor increases when the same acceleration rate is used in individual coils. The majority of the studies on MB-EPI have used a receiver coil having 32 or more channels in a 3 Tesla MRI and a 7 Tesla ultra-high field MRI. We used a 1.5 Tesla MRI and a 12-channel receiver coil. As a result, image degradation was induced by a decreased SNR and an increased g-factor as well as the effect of the L-factor. Statistically significant differences were observed between the MB-EPI-based imaging (MB-short and MB-MPG) and the conventional imaging (ref. DKI).

The MK showed a statistically significant difference from the conventional method with the equipment and imaging conditions used in this study. However, a new technique to decrease the L-factor has been reported [22], and the present results may be improved in the future. We expect that future improvements to the 1.5 Tesla MRI will result in statistically insignificant differences from the conventional method.

Conclusion

We evaluated the effect of the combination of MB-EPI with

DKI using a 1.5 Tesla MRI and a 12-channel receiver coil. Apparent artifact and image degradation were not observed, while statistically significant differences from the conventional method were detected by pyramidal tract-specific analysis. MB-EPI shortens acquisition time up to 37.2%, and therefore the combination with DKI, which requires a longer acquisition time than that of general DWI, may be useful in clinical applications. This method is effective in qualitative evaluation; however, careful attention is required for quantitative evaluation because SNR decreases depending on the MRI equipment and receiver coil used and the g-factor and L-factor significantly affect image quality.

References

1. Mansfield P, Pykett IL. Biological and medical imaging by NMR. J Magn Reson. 1978; 29: 355-373.
2. Stejskal E O, Tanner JE. Spin Diffusion Measurements: Spin Echoes in the Presence of a Time-Dependent Field Gradient. J Chem Phys. 1965; 42: 288-292.
3. KunimatsuA, Aoki S, Masutani Y, Abe O, Hayashi N, Mori H, et al. The Optimal trackability threshold of fractional anisotropy for diffusion tensor tractography of the corticospinal trac. Magn Reson Med Sci. 2004; 3: 11-17.
4. Sotak CH. The role of diffusion tensor imaging in the evaluation of ischemic brain injury – a review. NMR Biomed. 2002; 15: 561-569.
5. Latt J, Nilsson M, Westen DV, Wireatam R, Stahlberg F, Brockstedt S. Diffusion-weighted MRI measurements on stroke patients reveal water-exchange mechanisms in sub-acute ischaemic lesions. NMR Biomed. 2009; 22: 619-628.
6. Callaghan PT, Coy A, Macgowan D, Packer KJ, Zelaya FO. Diffraction like effects in NMR diffusion studies of fluids in porous solids. Nature. 1991; 351: 467-469.
7. Jensen JH, Helpern JA, Ramani A, Lu H, Kaczynski K. Diffusion kurtosis imaging: the quantification of non-gaussian water diffusion by means of magnetic resonance imaging. Magn Reson Med. 2005; 53:1432-1440.
8. Hori M, Fukunaga I, Masutani Y, Taoka T, Kamagata K, Suzuki Y, et al. Visualizing Non-Gaussian Diffusion: Clinical Application of q-Space Imaging and Diffusional Kurtosis Imaging of the Brain and Spine. Magn Reson Med Sci. 2012; 11: 221-233.
9. Raab P, Hattingen E, Franz K, Zanella FE, Lanfermann H. Cerebral gliomas: diffusional kurtosis imaging analysis of microstructural diffurences. Radiology. 2010; 254: 876-881.
10. Pruessmann KP, Weiger M, Scheidegger MB, Boesiger P. SENSE: Sensitivity Encoding for Fast MRI. Magn Reson Med. 1999; 42: 952-962.
11. Nunes RG, Hajnal JV, Golay X, Larkman DJ. Simultaneous slice excitation and reconstruction for single shot EPI. Proceedings of the 14th Annual Meeting of ISMRM. 2006; 293.
12. Larkman DJ, Hajnal JV, Herlihy AH, Coutts GA, Young IR, Ehnholm G. Use of multicoil arrays for separation of signal from multiple slices simultaneously excited. J Magn Reson Imaging. 2001; 13: 313-317.
13. The Human Connectome Project. 2016.
14. Setsompop K, Cohen-Adad J, Gagoski BA, Raij T, Yendiki A, Keil B, et al. Improving diffusion MRI using simultaneous multi-slice echo planar imaging. Neuroimage. 2012; 63: 569-580.
15. Smith SM, Miller KL, Moeller S, Xu J, Auerbach EJ, Woolrich MW, et al. Temporally-independent functional modes of spontaneous brain activity. Proc Natl AcadSci USA. 2012; 109: 3131-3136.
16. Kannan RA, Shergill SS, Barker GJ, Catani M, Ng VW, Howard R, et al. Tract-specific anisotropy measurements in diffusion tensor imaging. Psychiatry Res. 2006; 146: 73-82.
17. Ugurbil K, Xu J, Auerbach EJ, MoellerS, Vu AT, Duarte-Carvajalino JM, et al. Pushing spatial and temporal resolution for functional and diffusion MRI in the Human Connectome Project. Neuroimage. 2013; 80: 80-104.
18. Xu J, Moeller S, Auerbach EJ, Strupp J, Smith SM, Feinberg DA, et al. Evaluation of slice accelerations using multiband echo planar imaging at 3T. Neuroimage. 2013; 83: 991-1001.
19. Setsompop K, Gagoski BA, Polimeni JR, Witzel T, Wedeen VJ, Wald LL. Blipped-controlled aliasing in parallel imaging for simultaneous multislice echo planar imaging with reduced g-factor penalty. Magn Reson Med. 2012; 67: 1210-1224.
20. Grismold MA, Jakob PM, Heidemann RM, Nittka M, Jellus V, Wang J, et al. Generalized autocalibrating partially parallel acquisitions (GRAPPA). Magn Reson Med. 2002; 47: 1202-1210.
21. Wiggins GC, Polimeni JR, Potthast A, Schmitt M, Alagappan V, Wald LL. 96 Channel receive only head coil for 3 Tesla: Design optimization and evaluation. Magn Reson Med. 2009; 62: 754-762.
22. Moeller S, Xu J, Auerbach EJ, Yacoub E, Ugurbil K. Signal Leakage(L-factor) as a measure for parallel imaging performance among simultaneously multi-Slice (SMS) excited and acquired signals. Proceedings of the 20th Annual Meeting of ISMRM. 2012; 519.

Citation: Kasahara A, Suzuki Y, Mitsuda M, Yoshikawa K, Hori M, Maruyama K, et al. Usefulness and Consideration of Multi-Band EPI using Simultaneous Multi-Slice for Diffusion Kurtosis Imaging at 1.5 Tesla Magnetic Resonance Imaging. Austin J Radiol. 2016; 3(4): 1060.